Materials Science and Engineering B 176 (2011) 736–739

Contents lists available at ScienceDirect

Materials Science and Engineering B

journal homepage: www.elsevier.com/locate/mseb

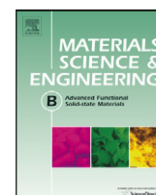

Ultraviolet photodetectors with MgZnO nanowall networks grown by molecular beam epitaxy on Si(1 1 1) substrates

Dayong Jiang [a], Jieming Qin [a,b,*], Xiyan Zhang [a], Zhaohui Bai [a], Dezhen Shen [c]

[a] School of Materials Science and Engineering, Changchun University of Science and Technology, Changchun 130022, China
[b] College of Physics and Electronic Information, Inner Mongolia National University, Tong liao 028043, China
[c] Key Laboratory of Excited State Processes, Changchun Institute of Optics, Fine Mechanics and Physics, Chinese Academy of Sciences, Changchun 130033, China

ARTICLE INFO

Article history:
Received 21 November 2010
Received in revised form 22 February 2011
Accepted 1 March 2011

Keywords:
MgZnO
Nanowall
Photodetector
MSM
Responsivity

ABSTRACT

$Mg_{0.05}Zn_{0.95}O$ nanowall networks ultraviolet (UV) photodetector was fabricated on Si(1 1 1) by plasma-assisted molecular beam epitaxy. Based on the $Mg_{0.05}Zn_{0.95}O$ nanowall networks, planar geometry photoconductive type metal–semiconductor–metal photodetector was fabricated. At 5 V bias, the peak responsivity of 24.65 A/W was achieved at 352 nm, corresponding to an external quantum efficiency of ~8490%. Such high external quantum efficiency was attributed to the photoconductive gain, which can be explained by the presence of oxygen-related hole-trap states at the nanowall surface. The response time of 25 ms was determined by the measurements of photocurrent versus modulation frequency.

Published by Elsevier B.V.

1. Introduction

In the past years, much effort has been devoted to research on MgZnO material system for their promising optoelectronic application in ultraviolet (UV) regions [1–3]. A number of reports on photoconductive [4], MSM [5], and *p*–*n* junction [6] UV detectors have been reported in the literature. While the vast majority of these photodetectors were fabricated from epilayers grown on sapphire substrates by pulse laser deposition (PLD) [5,7], only a few utilized on Si as the substrate [8] and fewer grew epilayers by molecular beam epitaxy (MBE). Nevertheless, the use of silicon offers many benefits: large area, low-cost, highly perfect substrates are readily available, a very sophisticated backside process technology has been developed over many years, and thermal expansion mismatch between detector arrays and read-out electronics would be mitigated.

The photodetectors based on nanostructure materials usually present high responsivity, which is attributed to the large surface-to-volume ratio, and photoconductive gain. ZnO-based nanostructures are regarded as one of the most promising materials for UV photodetectors [9,10]. No information can be found on MgZnO nanostructures UV photodetectors on Si substrates, to the best of our knowledge. In this letter, we report on the $Mg_xZn_{1-x}O$ nanowall networks on Si(1 1 1) by MBE. $Mg_xZn_{1-x}O$ nanowall networks MSM photodetectors are fabricated, and the resultant optical and electrical properties of the photodetectors are also discussed.

2. Experiments

The growth was carried out using a MBE system equipped with Knudsen cell for a Zn solid source (99.9999%) and an Mg solid source (99.999%) and radio frequency (RF) plasma source for oxygen. The background vacuum of the growth chamber was about 1×10^{-7} Pa with a liquid nitrogen supply. During the growth, the RF power of oxygen plasma was 300 W, the flow rate was kept at 2.0 sccm, and beam fluxes pressures of Zn and Mg were 3.0×10^{-3} and 2.0×10^{-5} Pa, respectively. Epitaxial layer growth was performed at a substrate temperature of 600 °C, and the temperature was monitored using pyrometer. In order to obtain a clean fresh surface, the Si substrate was etched in H_2O:HCl:H_2O_2 (1:3:1) solution, and then oxide was removed in a dilute HF water solution.

X-ray diffraction (XRD) spectra were collected with a D/max – RA X-ray spectrometer (Rigaku International Corp., Japan) with CuKα radiation of 1.543 Å to obtain the structural information. The surface morphology was observed by using a A Hitachi S4800 scanning electron micrograph (SEM). The current–voltage (*I*–*V*) characterization was measured by a Hall effects measurement system.

A standard lock-in amplifier technique was employed for the spectral response measurements, where a 150 W xenon lamp was

* Corresponding author at: School of Materials Science and Engineering, Changchun University of Science and Technology, Changchun 130022, China. Tel.: +86 431 85583016; fax: +86 431 85583015.
E-mail address: qjmqh@sohu.com (J. Qin).

0921-5107/$ – see front matter. Published by Elsevier B.V.
doi:10.1016/j.mseb.2011.03.001

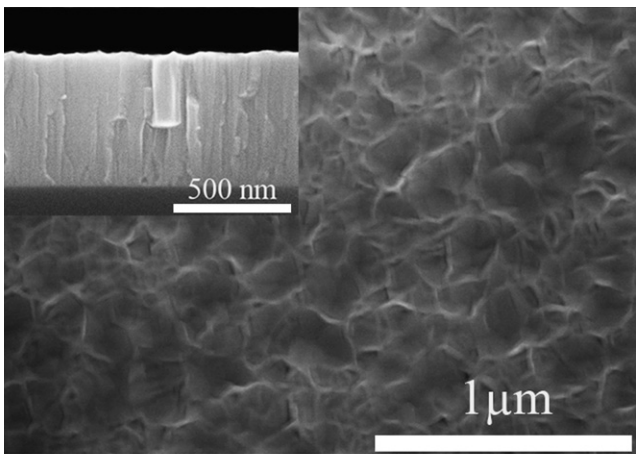

Fig. 1. FE-SEM image of PAMBE-grown MgZnO nanowall networks on Si(1 1 1) substrate. The inset shows the cross-sectional FE-SEM image of the MgZnO nanowall networks on Si(1 1 1) substrate.

used. The photodetector was illuminated from the front side. Using an intensity-modulated optical signal, which was produced using a mechanical chopper in the beam path of the xenon light, the response time of the photodetector was also measured.

3. Results and discussion

Fig. 1 shows field-emission scanning electron microscope (FE-SEM) image of MgZnO nanowall networks grown on Si(1 1 1) substrate. In the SEM image for the sample, the wall structure on the substrate was observed, and that the inner diameters of the nanowalls typically range from 100 to 500 nm. A large number of nanowalls with extremely small thicknesses were below 25 nm. It should be pointed out that the average thickness of MgZnO nanowall networks is much smaller than that in the previous reports [11]. As shown in the inset of Fig. 1, an MgZnO thin film with an average thickness of 600 nm formed between the Si(1 1 1) substrate and MgZnO nanowalls.

Fig. 2 shows the X-ray diffraction (XRD) of MgZnO film grown on Si(1 1 1) substrate. The appearance of only (0 0 0 2) peak in Fig. 2 indicates that the film is highly *c*-axis oriented and corresponds to (0 0 0 2) orientation of the MgZnO hexagonal structure. The XRD spectrum of pure ZnO has also been shown for comparison. It should be noted that the full-width-half-maximum (FWHM) of our MgZnO XRD peak is 0.2°. Such small XRD FWHM suggests that the crystal quality of our MgZnO film was reasonably good. In order to better understand the Mg composition in the MgZnO nanowall networks and the MgZnO thin film, energy-dispersive X-ray spectroscopy (EDS) measurements for the above areas were carried out. It was observed that the Zn/Mg ratio in both areas were almost the same, and the Mg composition in the nanowall networks is about 5%.

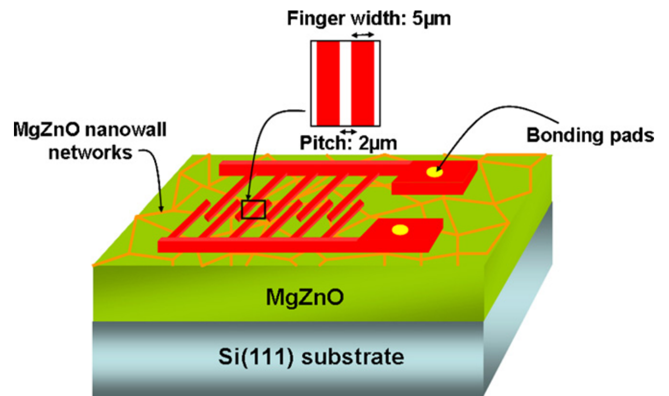

Fig. 3. Schematic full view of the interdigitated contacts including the values of the finger width and the pitch.

The MSM structure was fabricated on $Mg_{0.05}Zn_{0.95}O$ nanowall networks using an interdigitated electrode mask set. Schematic full view of the interdigitated electrodes is shown in Fig. 3. The electrode fingers are 5 μm wide, 500 μm long, and on a pitch of 2 μm. A 200 nm thick Au was deposited by using vacuum resistance evaporation with a growth rate of approximately 50 nm/min. The MSM electrodes were then fined by a lift-off process. After further lithography, a 500 nm thick indium layer was deposited by vacuum resistance evaporation. The *I–V* characteristics of the contacts were measured to be linear, indicating that they were Ohmic contacts, as shown in Fig. 4. The *I–V* curve under illumination at 360 nm was also shown for comparison. The typical resistance without illumination of the $Mg_{0.05}Zn_{0.95}O$ photodetetor was about 2 kΩ. Furthermore, the results of Hall measurement also indicated the mobility of the $Mg_{0.05}Zn_{0.95}O$ nanostructure was 1.1 cm^2/Vs, and the carrier concentration was about $5.6 \times 10^{18}/cm^3$ with n type conductivity.

Fig. 5 presents the responsivity as a function of wavelength for $M_{0.05}Zn_{0.95}O$ nanowall networks UV photodetector. The incident optical power was measured with a calibrated UV-enhanced Si photodetector. In the UV spectral region, the photodetctor showed a high responsivity, with only a little decrease from 352 to 200 nm. At 5 V bias, the peak response was found at 352 nm with the responsivity of 24.65 A/W, corresponding to an external quantum efficiency

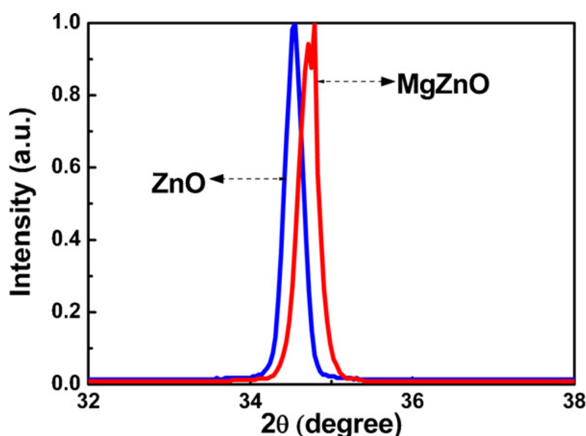

Fig. 2. XRD spectra of the MgZnO nanowall networks and pure ZnO on Si(1 1 1) substrate.

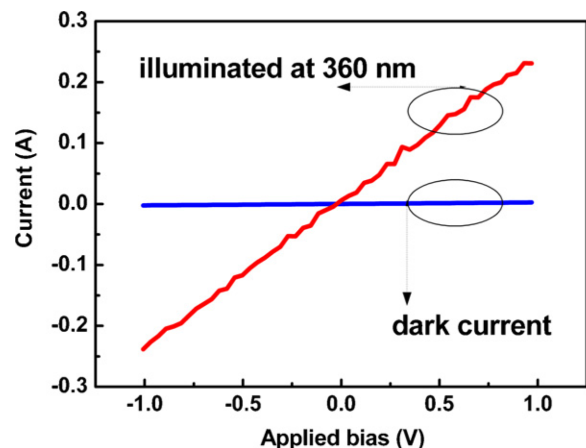

Fig. 4. *I–V* curves of dark current and illuminated at 360 nm.

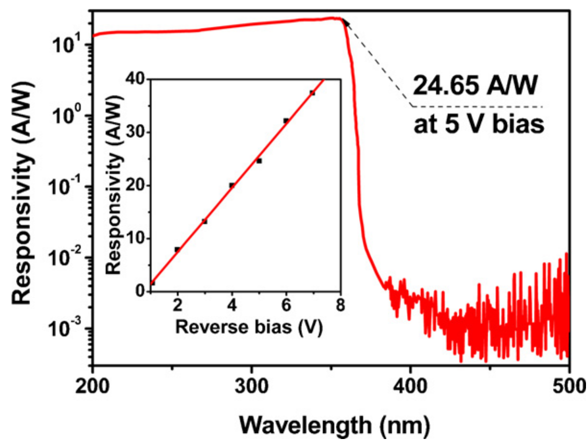

Fig. 5. Spectral response of the $Mg_{0.05}Zn_{0.95}O$ nanowall networks UV photodetector with the reverse of 5 V. The inset shows the responsivity at 352 nm as a function of reverse bias.

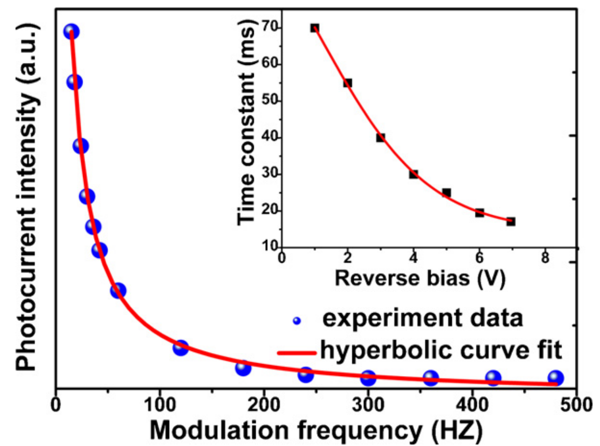

Fig. 6. Dependence of the photocurrent on the chopper frequency. The solid curve is the best fit curve. The inset is the dependence of the response time on the reverse bias of $Mg_{0.05}Zn_{0.95}O$ nanowall networks UV photodetector.

of ~8490%. The responsivity of our device was higher than that observed from other ZnO-based UV photodetectors on Si substrate [8,12,13]. The cutoff wavelength occurred at 360 nm. Meanwhile, the visible rejection (R352 nm/R400 nm) was more than four orders of magnitude, indicating a high degree of visible blindness. To further characterize the photodetectors, the responsivity as a function of reverse bias was determined. As shown in the inset of Fig. 5, a linear relationship was obtained between 1 and 7 V, indicating that no carrier mobility saturation even up to 7 V reverse bias.

It should be noted that such high external quantum efficiency was attributed to the photoconductive gain in the device. In our case, it was supposed that the gain can be explained by the presence of oxygen-related hole-trap states at the nanowall surface [14–16]. The trapping mechanism can be described as the oxygen molecules are adsorbed on the oxide surface and capture the free electrons present in the n-type oxide semiconductor. The photogenerated holes discharge the negatively charged adsorbed oxygen ions, and consequently, oxygen is photodesorbed from the surface, the unpair electrons are either collected at the anode or recombine with holes. The essential reaction formula can be shown as the following:

$$O_2(g) + e^- \rightarrow O_2^-(ad) \quad (1)$$

$$h\nu \rightarrow e^- + h^+ \quad (2)$$

$$h^+ + O_2^-(ad) \rightarrow O_2(g) \quad (3)$$

It is well known that when the oxygen molecules were adsorbed at the surface, it can produce an electron-depleted space-charge layer in the surface region. It is interesting to be noted that the resistance of $M_{0.05}Zn_{0.95}O$ naonowall was enhanced about 0.5 kΩ after applied voltages for a moment. The thermal effect is helpful to improve the absorption efficiency of oxygen molecules. Thus, the existence of oxygen-related hole-trap states at the surface was indirectly proved. To full understand these phenomena, we need to perform more experiments, such as the measurements in different oxygen concentrations and different temperatures. These experiments are underway and the results will be reported separately.

The dependence of photocurrent on the modulation frequency of the incident optical signal was also analyzed. The photocurrent decayed with the increase of the modulation frequency, as shown in Fig. 6. The plot showed a hyperbolic type relationship between the photocurrent and the modulation frequency [17]. From the plot, a response time of 25 ms was obtained at about 5 V bias. We plotted the response time dependence on the reverse bias of the $M_{0.05}Zn_{0.95}O$ nanowall networks UV photodetector from the experimental data, as shown in the inset of Fig. 6. The response time decreases with increasing reverse bias of the device, agreeing well with the effect of the sweep-out field increase. It should be noted that the response time of 25 ms is fall smaller than that reporter from ZnO-based MSM photodetectors [18].

4. Conclusions

In summary, the visible-blind $Mg_{0.05}Zn_{0.95}O$ nanowall networks UV photodetector has been fabricated on Si(1 1 1) by MBE. The photodetector exhibited a sharp cutoff wavelength at 360 nm. The peak responsibity of 24.65 A/W at 352 nm was measured at 5 V bias, corresponding to an external quantum efficiency of ~8490%. The visible rejection (R352 nm/R400 nm) was obtained more than four orders of magnitude from the fabricated photodetector. The photoconductive gain can be explained by presence of oxygen-related hole-trap states at the nanowall surface. The response time of 25 ms was determined by the measurements of photocurrent versus modulation frequency.

Acknowledgments

This work is supported by the National Natural Science Foundation of China (Grant No. 50772016), Scientific and Technological Development Project of Jilin Province, China (Grant No. 201101103), and Natural Science Foundation of Inner of Mongolia, China (Grant No. 2010MS0105).

References

[1] Z.K. Tang, P. Yu, G.K.L. Wong, M. Kawasaki, A. Ohtomo, H. Koinuma, Y. Segawa, Solid State Commun. 103 (1997) 459.
[2] S. Liang, H. Shen, Y. Liu, Z. Huo, Y. Lu, H. Shen, J. Cryst. Growth 225 (2001) 110.
[3] Q.A. Xu, J.W. Zhang, K.R. Ju, X.D. Yang, X. Hou, J. Cryst. Growth 289 (2006) 44.
[4] D.Y. Jiang, J.Y. Zhang, K.W. Liu, Y.M. Zhao, C.X. Cong, Y.M. Lu, B. Yao, Z.Z. Zhang, D.Z. Shen, Semicond. Sci. Technol. 22 (2007) 687.
[5] W. Yang, R.D. Vispute, S. Choopun, R.P. Sharma, T. Venkatesan, H. Shen, Appl. Phys. Lett. 78 (2001) 2707.
[6] K.W. Liu, D.Z. Shen, C.X. Shan, J.Y. Zhang, B. Yao, D.X. Zhao, Y.M. Lu, X.W. Fan, Appl. Phys. Lett. 91 (2007) 201106.
[7] S.S. Hullavarad, S. Dhar, B. Varughese, I. Takeuchi, T. Venkatesan, R.D. Vispute, J. Vac. Sci. Technol. A 23 (2005) 982.
[8] K. Koike, K. Hama, I. Nakashima, G.Y. Takada, K.I. Ogata, S. Sasa, M. Inoue, M. Yano, J. Cryst. Growth 278 (2005) 288.
[9] J.B.K. Law, J.T.L. Thong, Appl. Phys. Lett. 88 (2006) 133114.
[10] C.Y. Lu, S.J. Chang, S.P. Chang, C.T. Lee, C.F. Kuo, H.M. Chang, Y.Z. Chiou, C.L. Hsu, I.C. Chen, Appl. Phys. Lett. 89 (2006) 153101.
[11] H.T. Ng, J. Li, M.K. Smith, P. Nguyen, A. Cassell, J. Han, M. Meyyappan, Science 300 (2003) 1249.
[12] C.H. Park, I.S. Jeong, J.H. Kim, S. Im, Appl. Phys. Lett. 82 (2003) 3973.

[13] I.S. Jenong, J.H. Kim, S. Im, Appl. Phys. Lett. 83 (2003) 2946.
[14] Q.H. Li, T. Gao, Y.G. Wang, T.H. Wang, Appl. Phys. Lett. 86 (2005) 123117.
[15] Y.W. Heo, B.S. Kang, L.C. Tien, D.P. Norton, F. Ren, J.R. LaRoche, S.J. Pearton, Appl. Phys. A: Mater. Sci. Process 80 (2005) 497.
[16] O. Harnack, C. Pacholski, H. Weller, A. Yasuda, J.M. Wessels, Nano Lett. 70 (1997) 3516.
[17] B. Shen, K. Yang, L. Zang, Z.Z. Chen, Y.G. Zhou, P. Chen, R. Zhang, Z.C. Huang, H.S. Zhou, Y.D. Zheng, Jpn. J. Appl. Phys., Part 1 38 (1999) 767.
[18] H.K. Yadav, K. Screenivas, V. Gupta, Appl. Phys. Lett. 90 (2007) 172113.